A98-31633

ICAS-98-5,3,4

AN IMPROVED FATIGUE APPROACH FOR DESIGNING AIRCRAFT JOINTS

Duprat, D., Journet, B., Ithurralde, C.
Aerospatiale, France

Abstract

One of the major fatigue problems in airplanes takes place at fasteners holes of junctions. The AIRBUS partner companies mainly resort to efficient technologies such as interference fitting or cold working.

The know how in design to take these benefits into account is still very pragmatic. In order to better optimise the design, there is a need to improve the predictive tools and reduce the number of necessary tests. In this respect, this paper proposes simple approaches to predict the fatigue behaviour of cold worked fastener holes for fatigue and damage tolerance design. The rationale is based on the way the residual stresses induced by these technological processes, which are the source of benefit, is dealt with.

Tests are carried out in order to review the mechanical grounds of the modelling. A retardation coefficient is proposed for the prediction of crack growth.

In addition, this paper emphasises a theoretical approach to predict crack initiation and propagation.

Introduction

The design of cold worked fastener holes is still very pragmatic and relies too much on large series of tests. There is a need to better rationalise the results and know how to take into account the beneficial residual stresses. This paper addresses crack initiation and crack propagation in cold worked holes.

As far as crack initiation is concerned, much effort was placed during the last few years at Aerospatiale on developing fatigue prediction capabilities. The paper only presents the theoretical output of the work with reference to the experimental testing programmes that helped in validating the model. The feature is that the analysis must proceed with non proportional multiaxial loading.

As far as crack propagation is concerned, the effort is still ongoing at Aerospatiale. The paper focuses on the experimental test to highlight the mechanical understanding of crack propagation in cold worked holes. At this stage a straightforward analysis with retardation coefficient is presented. Improvement must proceed with 3D finite element analysis and stress relaxation.

The paper is broken down into two parts :

- crack propagation : test and retardation coefficient analysis
- theoretical approach :
  - crack initiation prediction : presentation of the validated model
  - crack propagation prediction : guidelines to lay ground for the retardation coefficient analysis.

Crack propagation test programme

Test specimens

The specimen geometry is shown in figure 1. The cut out is the same (50 x 250 x 2) for all the test series. Only the hole diameter changes. Three specimens per type were manufactured in L-T orientation.

The alloy under study is 7075T651 made out of 2 mm thin sheets.

Reference specimens. A through thickness flaw, 0.2 mm long, was machined on one side of the hole. This helps crack initiation and crack length monitoring on one side of the hole only throughout the test. The hole diameter is 6.22 mm.

Cold worked specimens. The hole was cold worked according to Aerospatiale procedure. The rate was 4%. The split bush was 0-180°/L oriented and the hole was not reamed before machining an initial flaw similar to that on the reference specimens. The hole diameter is 5.85 mm after cold working.

21st ICAS Congress
13-18 September 1998
Melbourne, Australia

Testing conditions

The fatigue tests are run under load control on a 100 kN INSTRON servohydraulic machine. The test frequency is set at 20 Hz and the R ratio is 0.1. The holes of reference and cold worked specimens are empty. The applied remote stress (gross stress) is 150 and 170 MPa in order to be in Paris regime.

The crack length is monitored on both sides of the specimens when necessary through an 8-100X travelling microscope. The accuracy is 10 μm.

Specimen baseline K data

The stress intensity factor is calculated using finite element analysis for a one sided through cracked hole reference specimen.

The results were compared to the analytical solution given by TADA and PARIS in the case of an infinite plate. The formulations agree up to a crack length of 8 mm. The finite element result is fitted to the following function :

$$K = \sigma/10\ (\alpha_0 a^0+\alpha_1 a^1+\alpha_2 a^2+\alpha_3 a^3)$$

K (MPa.m$^{1/2}$),
σ (MPa), gross stress,
a (mm), crack length from the hole edge.

The value of α_i are given in the following table for different ranges of crack length :

a (mm)	0 – 0.6	0.6 - 2	>2
α_0	0	0.77	0.84
α_1	5.97	0.67	0.25
α_2	-12.73	-0.29	-0.029
α_3	9.62	0.04	0.0013

Material baseline data

In order to assess the crack growth behaviour at holes, reference data are used.

Baseline fatigue crack growth rate data on 7075 T651 under an R ratio of 0.1 are taken from Aerospatiale data handbook. Within the range of ΔK values of concern in this study (10-30 MPa.m$^{1/2}$), it is appropriate to use Paris' law.

Material	C	m
7075 T651	4.68 10^{-7}	2.58

da/dN (mm/cycle)
ΔK (MPa.m$^{1/2}$)

Test results

Reference specimens. The crack growth measurements are plotted against the crack length, this latter one includes the bore radius.

The crack growth rate is taken as the linear intercept between two neighbouring data points.

The crack does initiate on the initial flaw and is fully through the thickness. Nothing happens on the other side of the bore until failure of the specimens.

The crack growth rates relative to the applied two stress levels are roughly in their ratio raised to Paris' law exponent :

$$(\frac{170}{150})^{2.58} = 1{,}38$$

Cold worked (CW) specimens. Crack initiation takes place all along the initial flaw. Then crack propagation takes on as a corner crack growth. It grows on the front face (entrance face of the mandrel) and stalls on the other one (back face) until the corner crack tears through this latter face at a distance approximately equal to 2 or 3 mm from the bore edge. At this stage, the crack turns into a through crack.

The fractographic examinations illustrate these different stages (figure 2). There is no crack initiation on the other side of the bore.

The front face was monitored in the early stage.

There is a large stress effect. The cycles numbers to crack initiation is too small to explain the differences.

Test Type	Specimen	Maximum fatigue stress	Cycles to crack initiation
Ref	AM1	150	1147
	AM2	150	739
	AM3	170	651
CW	AM7	170	3900
	AM8	150	7090
	AM9	150	15088

Figures 3 and 4 show the results obtained on samples AM7, AM8, AM9. . The front face crack growth is reported. The minimum crack growth rate is reached at about 1.5 mm from the hole edge for each testing test.

The data are compared with the reference tests for each applied fatigue stress level. The retardation is more significant under 150 MPa than under 170 MPa. The effect vanishes over a crack length of 8 or 9 mm which is about twice the hole radius.

The increasing and the decreasing parts of the retardation behaviour are fitted to the following shape function :

$$C = C_o(\frac{a}{d})^{\gamma}$$

With $C = da/dN_{cw} / da/dN_{Ref}$

a : distance from the hole edge

d, C_0 and γ are given for the decreasing and the increasing parts :

	150 MPa	170 MPa	
d (mm)	1.4	1.4	Decreasing part
C_o	0.001334	0.01355	
γ	-2.4050	-2.1355	
correlation	0.9972	0.9958	
d (mm)	4.18	3.1	Increasing part
C_o	0.2888	0.2580	
γ	3.6458	1.9949	
correlation	0.9221	0.9663	

Theoretical approach

Introduction

Test results have shown the retardation effect of technological processes such as cold working.

The aim of the following paragraph is to emphasise an approach witch allows to predict crack initiation and propagation. This prediction is based on the knowledge of the residual stresses.

Residual stress calculation

A 2D finite elements model was developed[1]. The cold working process is simulated by applying a radial nodal displacement of the hole edge (step 1) corresponding to 4% expansion. In a second step, the radial displacements are removed, simulating the removal of the mandrel (figure 5).

Since the residual stresses substantially vary through the plate thickness, hoop stress, axial stress and radial stress have been calculated (figure 6).

Crack initiation prediction

As the stress state is complex, a multiaxial fatigue model is required. Several formulae have been proposed, such as those of Sines[2], Crossland[3], or Dang Van[4].
For periodic in-phase loads, the predictions obtained using these equations comply with the experimental tendencies observed. Our multiaxial fatigue computation approach is based on Crossland's equation as it is easy to implement.

The formula proposed by Crossland is expressed as a linear combination of the equivalent shear stress amplitude and of the maximum hydrostatic stress reached during a load cycle:

$$T_{eqa} + B_N.P_{max} < A_N \qquad (1)$$

where:

A_N and B_N are parameters defined for fatigue life N
T_{eqa} is the equivalent shear amplitude,
P_{max} is the maximum hydrostatic stress.

Failure occurs when $(T_{eqa}+B_N.P_{max})$ equals A_N.

Definition of P_{max} and T_{eqa} The hydrostatic stress p(t) is equal to one third of the trace of the stress tensor $\Sigma(t)$.

An iteration over time is used to define the instant in time corresponding to maximum hydrostatic stress:

$$P_{max} = \frac{1}{3}\ max_{(t)}[trace\{\Sigma(t)\}] \qquad (2)$$

For any periodic load, the point representing the stress tensor $\Sigma(t)$ describes a closed curve (C_Σ) that we can call a load trajectory.

For radial (or proportional) loads, the load trajectory is a line segment passing through the origin. The principal axes of the stress tensor $\Sigma(t)$ are fixed during the cycle. In this case, the equivalent shear stress amplitude for a point on the structure is expressed as:

$$T_{eqa} = \sqrt{J_{2a}} \qquad (3)$$

where:

$$J_{2a} = \frac{1}{6}\ [(\sigma_{Ia}-\sigma_{IIa})^2+(\sigma_{Ia}-\sigma_{IIIa})^2+(\sigma_{IIa}-\sigma_{IIIa})^2] \qquad (4)$$

$$\sigma_{Ia}=(\sigma_{Imax}-\sigma_{Imin})/2$$
$$\sigma_{IIa}=(\sigma_{IImax}-\sigma_{IImin})/2 \quad (5)$$
$$\sigma_{IIIa}=(\sigma_{IIImax}-\sigma_{IIImin})/2$$

However, for our study (superposition of the external load and the effect due to the cold working process), the principal stress axes vary over time, as the load is not proportional.

In the most general case of non-proportional periodic loads, T_{eqa} is homogeneous to a distance in the deviatoric stress space. In fact, if we project the load trajectory (C_Σ) onto the deviatoric space, we also obtain a closed curve (C_S) (figure 7).

T_{eqa} is then expressed as:

$$T_{eqa}=\frac{1}{2}\frac{D}{\sqrt{2}} \quad (6)$$

D is the longest chord intercepting (C_S). In the deviatoric space, D is calculated as follows:

$$D=\max_{(t1,t2)}\sqrt{\text{trace}([S(t1)-S(t2)]^*[S(t1)-S(t2)])} \quad (7)$$

where: $S(t)=\Sigma(t)-p(t).Id$ (8)

$$Id=\begin{bmatrix}1&0&0\\0&1&0\\0&0&1\end{bmatrix}$$

Evalution of model parameters. The two parameters can be defined by means of two simple uniaxial tests. The tests selected here are a fully-reversed tension-compression test and a repeated tension (i.e. zero to tension) test :

Thus, we obtain equations (9) and (10) :

$$A_N=\frac{\sigma_0(N).\sigma_{-1}(N)}{2\sqrt{3}(\sigma_0(N)-\sigma_{-1}(N))}$$

$$B_N=\frac{3.(2.\sigma_{-1}(N)-\sigma_0(N))}{2\sqrt{3}(\sigma_0(N)-\sigma_{-1}(N))}$$

$\sigma_0(N)$ is the maximum stress (for R=0) corresponding to failure at N cycles.

$\sigma_{-1}(N)$ is the maximum stress (for R=-1) corresponding to failure at N cycles.

For economic reasons (weight and volume gain), calculations in civil aeronautics are generally made between low and high cycle fatigue, i.e. for lives on failure of between 10^4 and 10^7 cycles inclusive.

If, for this range of life, we plot experimental results, concerning an aluminium alloy, on a graph ($\log(s_{max})$,log(N)), we can observe that these points fall approximately on a straight line. From here on, it is possible to model fatigue cycle curves by means of straight lines.

The use of a specific point (corresponding to $N=10^5$ cycles) and the line gradient (-1/p) result in the following expressions:

$$\sigma_{-1}(N)=\sigma_{-1}(10^5).\left(\frac{10^5}{N}\right)^{1/p} \quad (11)$$

$$\sigma_0(N)=\sigma_0(10^5).\left(\frac{10^5}{N}\right)^{1/p} \quad (12)$$

Relations (11) and (12) are defined for a 50% probability of failure.

Introducing the above values of $\sigma_{-1}(N)$ and $\sigma_0(N)$ into equations (9) and (10), we obtain :

$$A_N=\frac{\sigma_0(10^5).\sigma_{-1}(10^5)}{2\sqrt{3}(\sigma_0(10^5)-\sigma_{-1}(10^5))}(10^5/N)^{1/P}$$

$$B_N=\frac{3.(2.\sigma_{-1}(10^5)-\sigma_0(10^5))}{2\sqrt{3}(\sigma_0(10^5)-\sigma_{-1}(10^5))}$$

Solving for N the Crossland formula, the fatigue life is obtained :

$$N=10^5.\left(\frac{\frac{\sigma_0(10^5).\sigma_{-1}(10^5)}{2\sqrt{3}(\sigma_0(10^5)-\sigma_{-1}(10^5))}}{Teqa+\frac{3.(2.\sigma_{-1}(10^5)-\sigma_0(10^5))}{2\sqrt{3}(\sigma_0(10^5)-\sigma_{-1}(10^5))}P\max}\right)^p$$

This approach is valid for any periodic loading : using discretised geometry, an elastoplastic computation gives the stress state at several instants during the load cycle.

It is consequently possible to define, on one hand, the maximum hydrostatic stress and, on the other

hand, the longest chord intercepting the load trajectory projected onto the deviatoric space (C_S). The last expression is used to deduce crack initiation period associated with each node in the model. (see figure 8)

Crack growth prediction

An 2D elastoplastic analysis of the stress field resulting from the combined residual and applied stresses is made. This allows to check the stress singularity beyond the plastic zone and calculate K at different crack length. The effect of the residual stresses is characterised as a coefficient relative to the straightforward calculation of the applied K.

The crack growth prediction (3D case in testing) is made on the surface of the specimen using this coefficient and the knowledge of the crack aspect ratio.

$$K_{remote+residual(3D)} = K_{remote(3D)} \cdot \frac{K_{remote+residual(2D)}}{K_{remote(2D)}}$$

$K_{remote(3D)}$ and $K_{remote(2D)}$ are given by the literature.

Using this expression, it is possible to determine the maximal value of the stress intensity factor K_{max}. The opening stress intensity factor K_{op} corresponds to the stress witch opens the crack.

Thus, the crack growth is deduced from Paris' law :

$$\frac{da}{dN} = C_{eff} . \Delta K_{eff}^{\ m} = C_{eff} . (K_{max} - K_{op})^m$$

Conclusion

The prime objective was to study fatigue behaviour with fastener hole technologies.

From the previous paragraphs, useful information can be highlighted for practical use.

Test results (crack propagation) :

- The crack initiation period is small since an initial flaw was machined.
- The improvements over the reference test are attributed to a large crack retardation effect. The improvement ratios are close to 10. This benefit mainly occurs during the first cracking millimeter. In this stage, the crack shape is that of a corner crack. The retardation is due to the very slow propagation through the thickness, related to a non uniform compressive residual stress distribution.
- The minimum crack growth rate is 2 to 3 orders of magnitude smaller than the reference one. The effect is operative over a distance about 2 times the hole radius. On cold worked samples, the minimum is reached when the crack has grown a distance of one half the hole radius.

Calculation approaches :

A model has been proposed in order to predict crack initiation period. It is based on the knowledge of the residual stresses induced by cold working.

An elastoplastic analysis of the stress field close to the crack tip leads to the prediction of Δk_{eff}. This value allows to calculate crack growth.

REFERENCES

(1) Fatigue crack growth in Aluminium alloys in the presence of residual stress introduced by cold working fastener holes.
C. Poussard, M. Poussard, Doctoral dissertation, University of Bristol, June 1994

(2) G. Sines, G. Ohgi, Trans. Am. Soc. Mech.Eng., J. Engng Mater. Techn., 103, 82-90, 1981

(3) B. Crossland, Proc. Int. Conf. Fatigue Metals, Intitution of Mechanical Engineers, London, 1956

(4) K. Dang Van, Mém. l'Artillerie française, 3, 641-722, 1973

(5) Fatigue life prediction of Interference fit fastener and cold worked holes.
D. Duprat, Int. J. Fatigue, Vol 18, n°8, pp 515-521, 1996

(6) Calculation of multiaxial fatigue for aeronautical applications..
D. Duprat, ECF 11, , 1995

(7) Propagation par fatigue de fissures bi et tridimensionnelles dans deux alliages d'aluminium. Effets de petite fissure et de chargements aléatoires.
A. Lefrançois, Doctoral dissertation, EMP, december 1987

(8) An evaluation of a fatigue crack growth prediction model of variable amplitude.
J. Schijve, TU Delf, report LR-537

(9) Elementary Engineering Fracture Mechanics.
D. Broek . Sijhoff & Noordhoff International Publishers B.V. – The Netherlands - Chapter 14. 1978

(10) The stress analysis of cracks handbook.
H. Tada, P. Paris, G. Irwin TU Delf, Del Research Corporation, Hellertown, Pennsylvania, 1973.

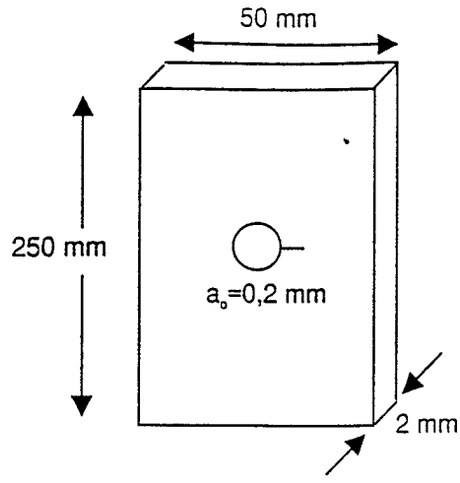

FIGURE 1 – Crack growth test specimen

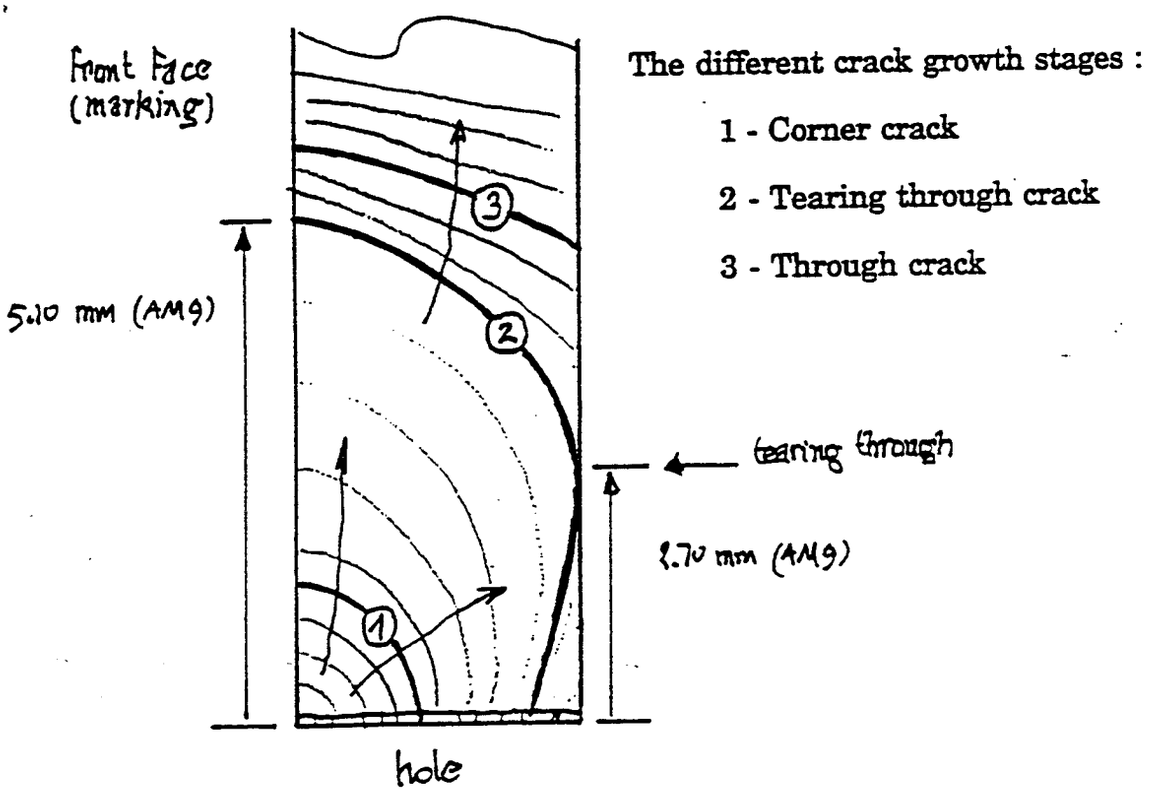

FIGURE 2 – Fractographic examination

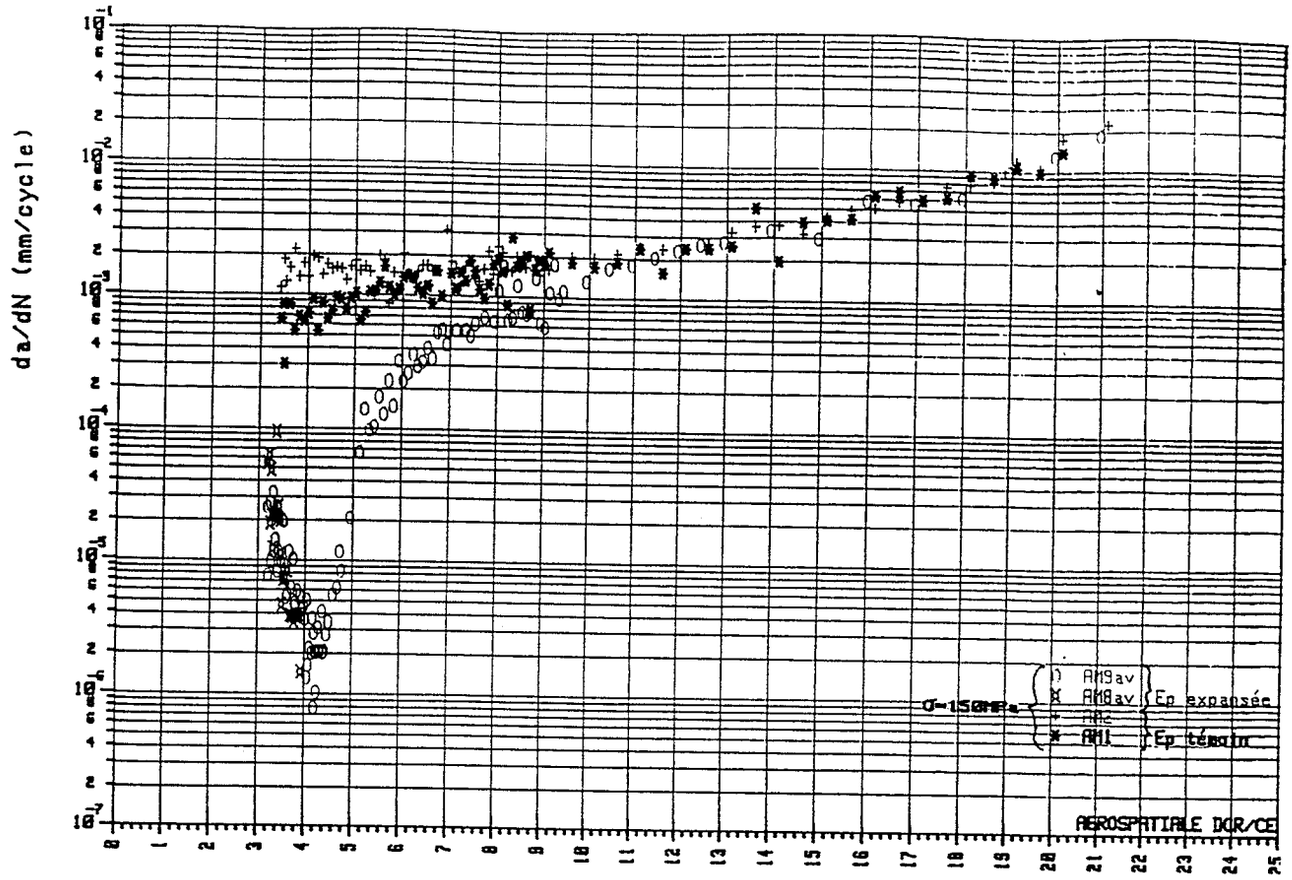

FIGURE 3 – Crack growth test result

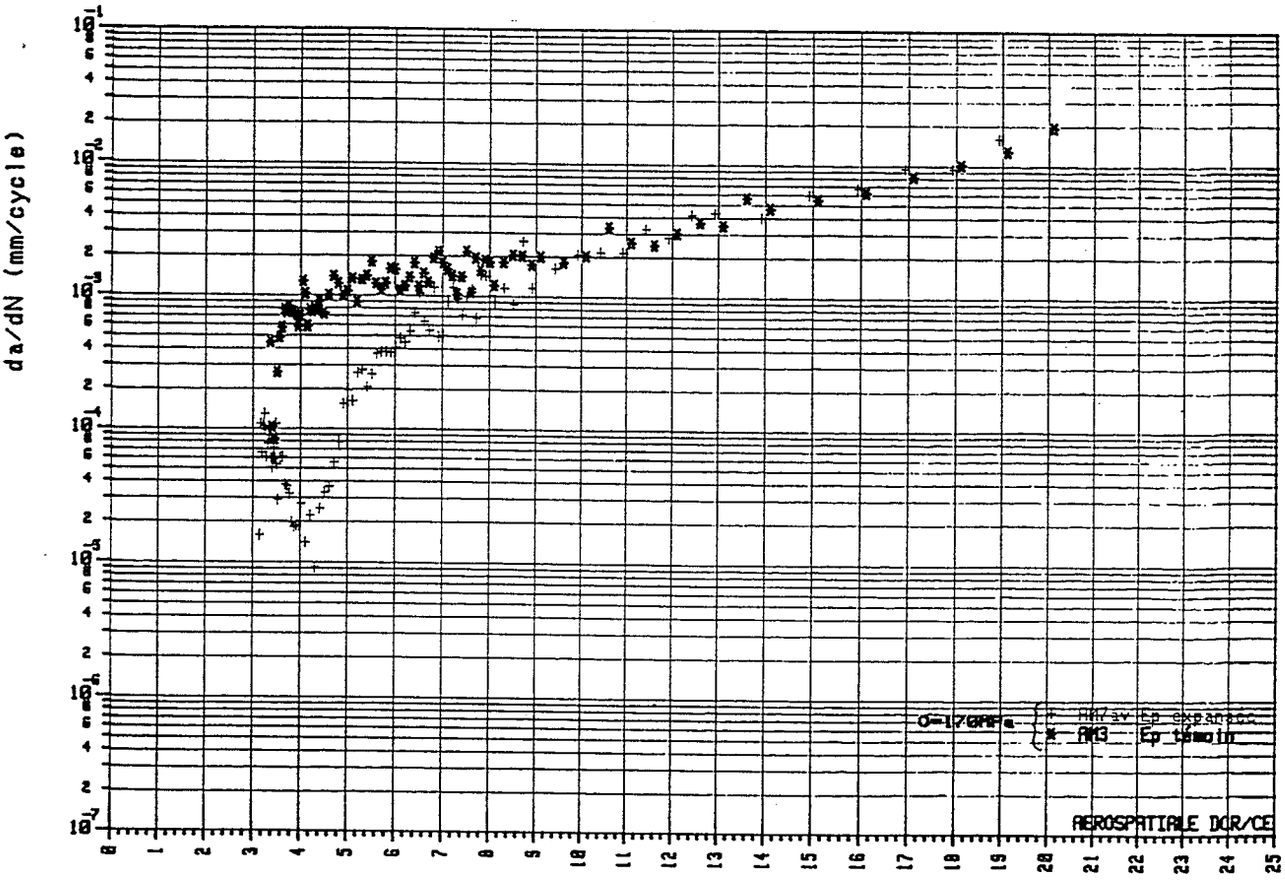

FIGURE 4 – Crack growth test result

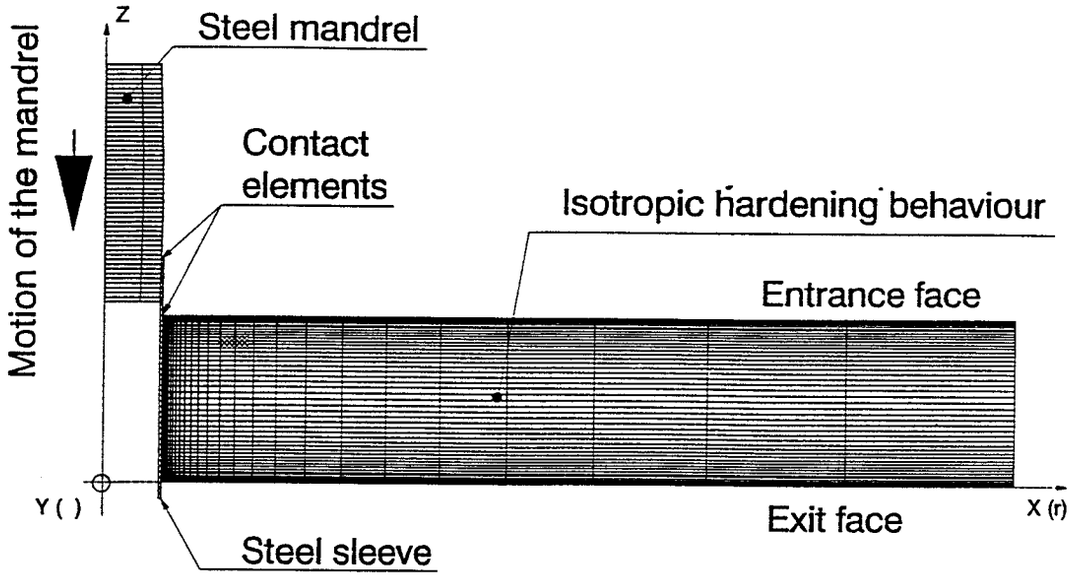

FIGURE 5 – Finite Elements Model of the cold working process

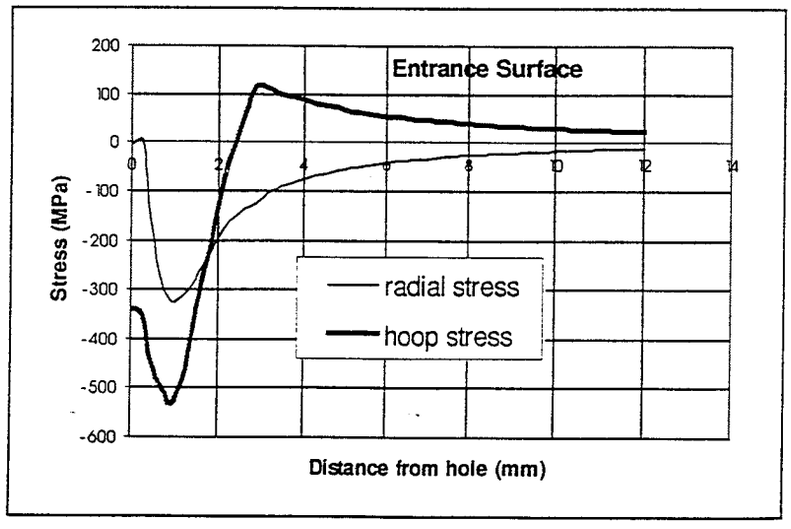

FIGURE 6a – Residual stress calculation (Entrance Surface)

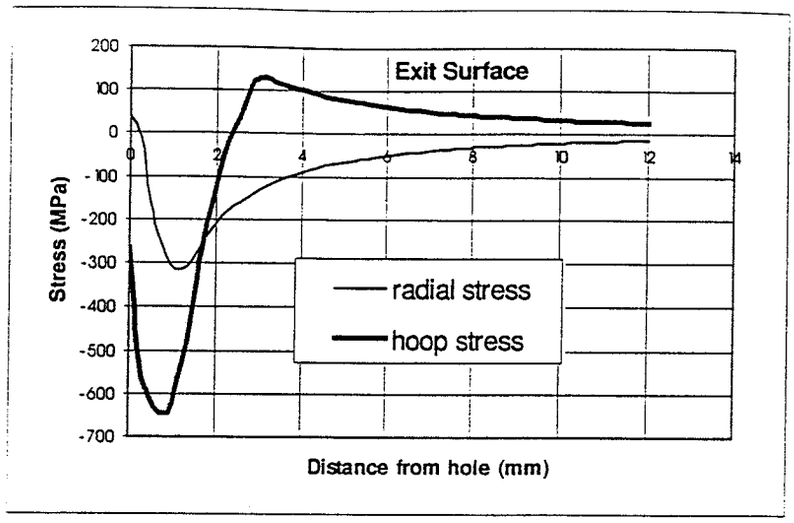

FIGURE 6b – Residual stress calculation (Exit Surface)

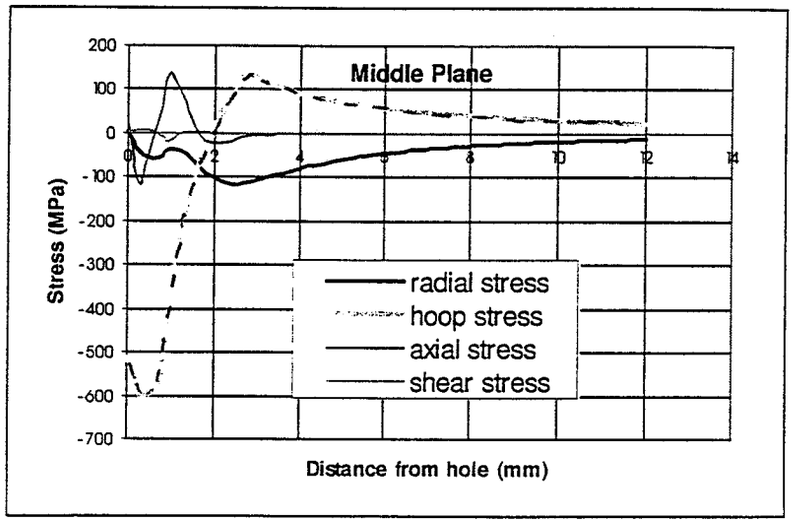

FIGURE 6c – Residual stress calculation (Middle Plane)

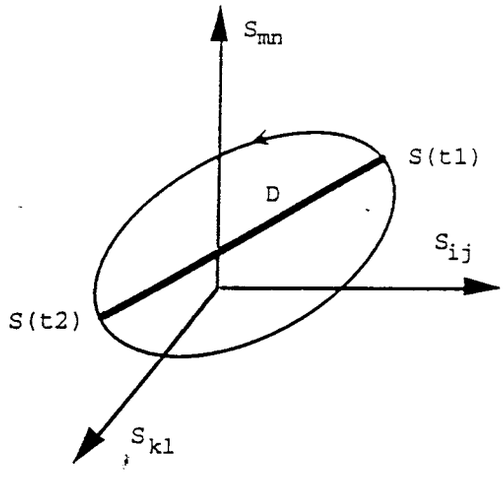

FIGURE 7 – Load trajectory in deflector hyperplane

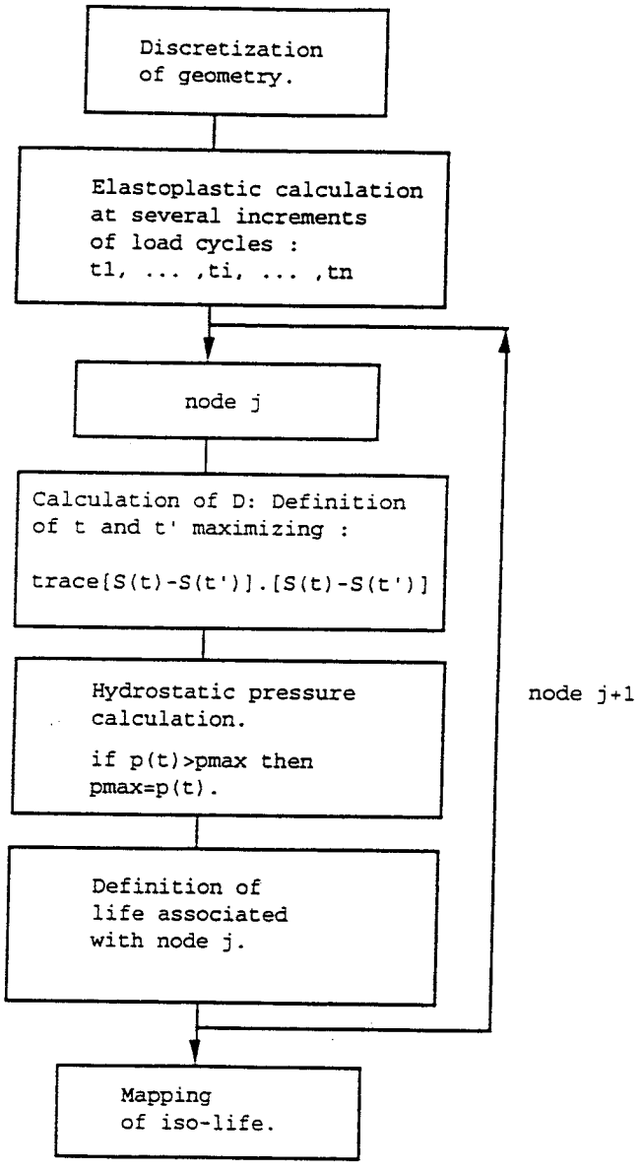

FIGURE 8 – Calculation approach for crack initiation